Numerical Experiments on the Near and Far Field of Acoustic and Elastic Waves Scattered by Cracks.

Carlos J. S. Alves
Centro de Matemática Aplicada, Instituto Superior Técnico,
Av. Rovisco Pais 1, 1049-001 Lisboa, Portugal

Summary

In this talk we will present some numerical experiments made with codes based on a boundary element method using a variational formulation for acoustic and elastic scattering by cracks on the three dimensional space. These experiments show the perturbation of the acoustic near and far field due to the change of the shape of the scattering obstacle and the possibilities of establishing criteria for detection. Similar experiments will be shown for three-dimensional elastic scattering. This work complements some of the numerical results already presented in [1], [2], [3], [4], [5].

Scattering by acoustic cracks

We consider the time-harmonic scattering problem in the resonance frequencies. Let Γ_1 and Γ_2 be two sound-hard flat cracks and take an acoustic incident plane wave of the form

$$u^{inc}(x) = e^{ikx\cdot d},$$

where $d \in S^2$, is an unitary direction that determines the direction of propagation of the acoustic wave. We also consider spherical waves centered in some point y, given by $u^{inc}(x) = \Phi(x-y)$, where Φ is the fundamental solution of the Helmholtz equation given by

$$\Phi(x) = \frac{e^{ik|x|}}{4\pi|x|}.$$

The scattered wave u verifies the Helmholtz equation, and we have the problem

$$\begin{cases} \Delta u + k^2 u = 0 & \text{in } \mathbf{R}^3 \backslash (\Gamma_1 \cup \Gamma_2) \\ \partial_n u = -\partial_n u^{inc} & \text{on } \Gamma_1 \cup \Gamma_2 \\ \partial_r u - iku = o(r^{-1}) & \text{when } r = |x| \to \infty \end{cases}$$

where the last condition is the Sommerfeld radiation condition. It is well known (e.g. [6]) that the behavior of the scattered wave can be described by the asymptotic relation

$$u(x) = \frac{e^{ikr}}{r} u_\infty(\hat{x}) + o(\frac{1}{r})$$

where $\hat{x} = \frac{x}{|x|} \in S^2$, and u_∞ is an analytic function with complex values defined on the unitary sphere S^2, called far field pattern.

It was proved in [7] that the solution of this problem can be given by the double layer potential

$$u(x) = \int_{\Gamma_1 \cup \Gamma_2} \partial_{n_y} \Phi(x-y)\varphi(y) ds_y,$$

where $\varphi \in H_{00}^{1/2}(\Gamma_1 \cup \Gamma_2)$ is a density that can be obtained by solving the following variational problem on the boundary (Hamdi formulation)

$$\int_{\Gamma_1 \cup \Gamma_2} \int_{\Gamma_1 \cup \Gamma_2} \Phi(x-y) \left(\text{curl}\ _\Gamma \varphi(x) \cdot \text{curl}\ _\Gamma \bar{\psi}(y) - k^2 \varphi(x) \bar{\psi}(y) \right) ds_y = - \int_{\Gamma_1 \cup \Gamma_2} \partial_n u^{inc}(x) \bar{\psi}(x) ds_x,$$

where the test functions ψ are taken in $H_{00}^{1/2}(\Gamma_1 \cup \Gamma_2)$. In this way it is possible to avoid the hypersingular kernel that would arise in the equation

$$-\partial_n u^{inc}(x) = \int_{\Gamma_1 \cup \Gamma_2} \partial_{n_x} \partial_{n_y} \Phi(x-y)\varphi(y) ds_y,$$

and one can proceed with the discretization using a finite element method (cf. [1]). We take a regular mesh of $\Gamma_1 \cup \Gamma_2$ and consider linear Lagrange finite elements, vanishing on the boundary of $\Gamma_1 \cup \Gamma_2$, therefore these test functions are in the space $H_{00}^{1/2}(\Gamma_1 \cup \Gamma_2)$.

In Figure 1 we plot an example of triangulation for two cracks in different planes. Γ_1 is a disk with radius 1 centered in the point $(0, 0, 1)$ and Γ_2 is of the same shape, but centered in $(-1, 0, 0)$.

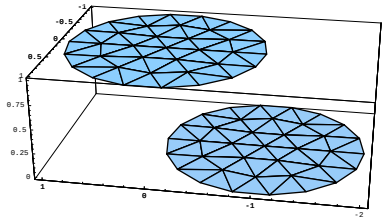

Figure 1: Two parallel cracks and the mesh used in the BEM.

• *Acoustic cracks in the same plane.* First we consider flat cracks in the same plane, Γ_1 and Γ_2 are disks with radius 1 with centers $(-2, 0, 0)$ and $(2, 0, 0)$, respectively. We took frequency $k = 4$ and two different spherical incident waves. In Figure 2 we plot out the results for a spherical wave centered in $y = (0, 0, 6)$, picture on the left, and for a spherical wave centered in $y = (-6, 0, 6)$, picture on the right. Notice that we only plot a cut, on the plane $x_2 = 0$, of the modulus of the amplitude, but the crack opening displacement is clearly visible. The first case corresponds to an almost normal incidence and the second case to an oblique incidence where the response of Γ_1, the closest crack to the point source y, is clearly bigger. One can also see that the direction of propagation of the scattered wave agrees with the reflection law, noticing that this is a case of small frequencies.

The same experiments can be taken in the asymptotic case, considering plane incident waves and measuring the far field pattern modulus. This is shown in Figure 3, where incidence direction d orthogonal to n, picture on the left, and with direction d making a 45 degree angle with the normal, picture on the center. In the picture on the right we plot the far field for a single crack (angle of 45 degrees). One can see that the global behaviors in the near field are transmited to the asymptotic situation. Comparing the case of a single crack with the case of two cracks, we can say that the amplitude is almost the sum of the two contributions, being the double in some directions and null on others. This explains that the number of lobs increases due to the interference of the scattered waves.

We also notice that in the direction corresponding to the plane of the crack, we have a null amplitude, which has been proven to be a characteristic that allows to identify the plane of the cracks (cf. [2], [4]).

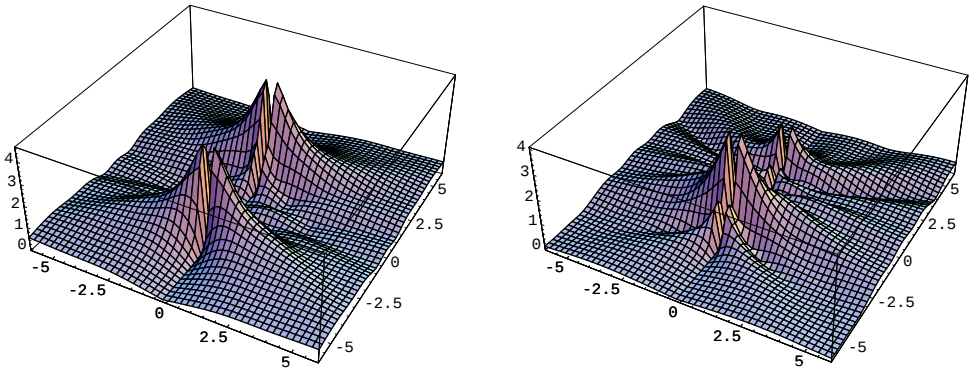

Figure 2: Near field amplitude for two cracks in the same plane.

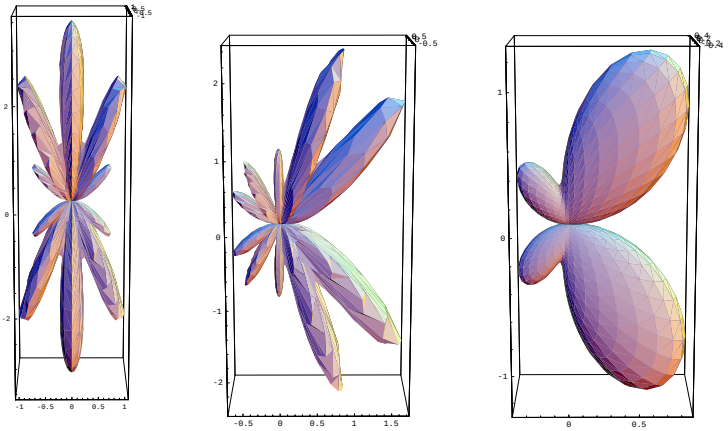

Figure 3: Far field patterns for two cracks in the same plane.

This characteristic is easily understood by noticing that in the case of plane cracks one gets from the double layer representation, that the kernel verifies

$$\partial_n \Phi(x-y) = n \cdot \nabla \frac{e^{ik|x-y|}}{4\pi|x-y|} = 0, \quad (x, y \in \Gamma)$$

because the gradient puts in evidence the term $x-y$ and when x and y are placed in the plane Γ (where Γ_1 and Γ_2 lie), $x-y$ is orthogonal to the normal n. The null amplitude in the plane directions is also true in the asymptotic situation. This characteristic is partially lost when Γ_1 and Γ_2 are in different planes, even if they are parallel. It is only partially lost, because it remains true in the far field, since parallel planes define the same asymptotic directions. This feature will be illustrated in the next examples.

• *Acoustic cracks in parallel planes.* Consider now the case those two same cracks in parallel planes. Γ_1 is now centered in $(0,0,0)$ and Γ_2 is centered in $(1,0,2)$. The wave scattered by the cracks after the incidence of a spherical wave centered in $(0,0,6)$ is plotted in Figure 4, on the left. The picture on the right corresponds to a spherical incident wave centered in $(-6,0,6)$. One can see that in the region between the two cracks interference phenomena occurs, and the scattered field becames more difficult to analyse. As pointed out before, in the near field the amplitude is not null in the plane of the cracks as it happened when the cracks were in the same plane.

In the asymptotic situation, we consider the same example, with incident plane waves and measure the far field. In Figure 5 we plotted the far field patterns for incident three different directions d. We

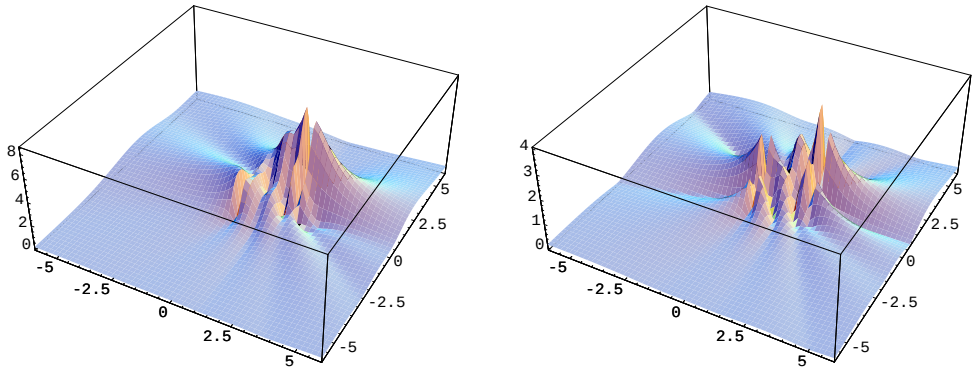

Figure 4: Near field amplitude for two acoustic cracks in parallel planes.

took a direction orthogonal to the cracks, picture on the left, another one making a 45 degree angle, picture on the center, and with a -45 degree, picture on the right. In the 3 situations the amplitude is null on the plane of the crack, as mentioned. We also notice that due to the non symmetric positions of the cracks, we do not have simmetry in the far field patterns.

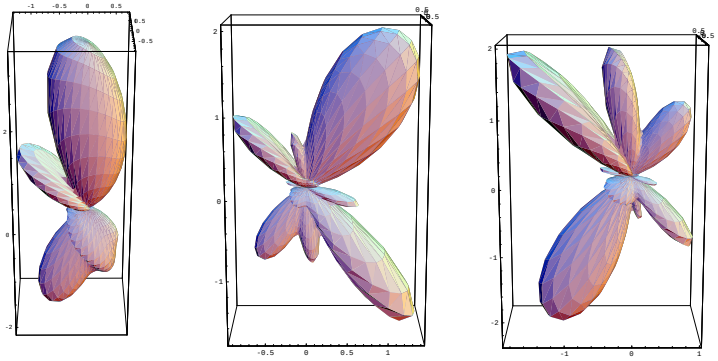

Figure 5: Far field amplitude for two acoustic cracks in parallel planes.

Scattering by elastic cracks

We just consider the case of the asymptotic behavior of scattering by two plane cracks in a 3D homogeneous and isotropic elastic medium.

Consider an elastic incident plane wave of the form

$$u^{inc}(x) = qe^{ikx\cdot d},$$

where $q, d \in S^2$, here d determines the direction of propagation of the acoustic wave and q the polarization. We have two types of waves, when $q = d$ they are called P-waves, and when $q \perp d$ they are called S-waves. The wavenumber k is $k_p = \frac{\omega}{\sqrt{\lambda+2\mu}}$ in the case of P-waves.and $k_s = \frac{\omega}{\sqrt{\mu}}$ in the case of S-waves, where λ, μ are the Lamé coefficients and ω is the frequency. The scattered wave u is a vector that verifies Navier equation, and in abbreviate notation we can state the problem

$$\begin{cases} \Delta^* u + \omega^2 u = 0 & \text{in } \mathbf{R}^3 \backslash (\Gamma_1 \cup \Gamma_2) \\ \partial_n^* u = -\partial_n^* u^{inc} & \text{on } \Gamma_1 \cup \Gamma_2 \\ \partial_r^* u - iKu = o(r^{-1}) & \text{when } r = |x| \to \infty \end{cases}$$

using the notation ∇^* for the stress tensor, defining $\Delta^* u = \nabla \cdot (\nabla^* u)$, and $\partial_n^* u = (\nabla^* u) n$, $\partial_r^* u = (\nabla^* u)\hat{x}$, $Ku = (\lambda + 2\mu) k_p (u.\hat{x})\hat{x} + \mu k_s (u - (u.\hat{x})\hat{x})$.

The fundamental solution is given by Kupradze's tensor and it was proved in [7], [8], [1] that the hypersingular integral equation arising from the double layer potential representation allows an equivalent boundary variational formulation, similar to the scalar acoustic case, but more complex. We have built a code adapted from the one used in [1] for the two cracks case (all experiments took less than a minute in an ordinary personal computer).

The asymptotic behavior of the scattered wave is now given by

$$u(x) = \frac{e^{ik_p r}}{r} u_\infty^P(\hat{x}) + \frac{e^{ik_s r}}{r} u_\infty^S(\hat{x}) + o(\frac{1}{r})$$

where u_∞^P is the P-far field, a vector with direction $\hat{x}$, and u_∞^S is the S-far field, a vector with direction orthogonal to $\hat{x}$. In the case of a flat crack we decompose the S-far field in two directions, the SH, on the plane of the crack, and the SV, orthogonal to the others. One criteria for detecting the crack (see also [5]) is given by searching the SH polarization direction q, since it verifies $q \cdot u_\infty^S(\hat{x}) = 0$ for all $\hat{x} \perp n$.

• *Elastic disk cracks in the same plane.* We consider Γ_1 centered in $(0,0,0)$ and Γ_2 centered in $(-2,0,0)$, both unitary disks, and the incidence of a P-elastic wave with propagation direction normal to the crack. We took frequency $\omega = 4$, and in Figure 6 the P and SV far field patterns are plotted. The SH far field is not plotted because it is null in this case. Comparing with the case of a single crack (not plotted) the number of lobs increases in this situation, especially in the SV far field.

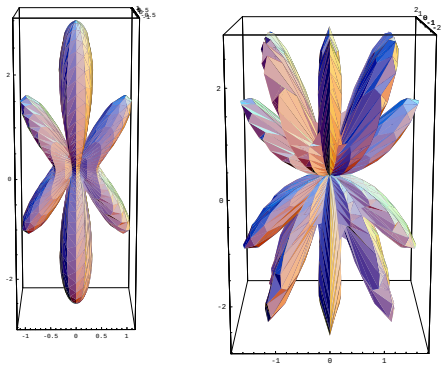

Figure 6: P and SV far field for two elastic cracks in the same plane.

• *Elastic disk cracks in parallel planes.* We consider Γ_1 centered in $(0,0,0)$ and Γ_2 centered in $(1,0,2)$, both unitary disks, and the incidence of a P-elastic wave with a propagation angle of 45 degrees, frequency $\omega = 4$, and we plot the P, SV and SH far field patterns in Figure 7. We notice that the scattered direction is particularly evident in the P-far field. In the SH far field we notice that the amplitude is null on the directions of the plane of the crack, as pointed out before.

• *Elastic elliptic cracks in parallel planes.* We consider Γ_1 an ellipse defined by radius $r_x = 1, r_y = \frac{1}{2}$, centered in $(0,0,0)$ and Γ_2 an ellipse with $r_x = \frac{1}{2}, r_y = 1$, centered in $(0,0,2)$. The incident plane wave is a P-wave with a propagation angle of 45 degrees.and the frequency is $\omega = 4$. Again, in Figure 8, we plot the P, SV, and SH far field patterns. The change in shape and location of both cracks does not affect the global aspect of the far fiel patterns, and we notice again the null SH far field in the plane of the crack, that can be used as a tool for identification of the cracks orientation.

Acknowledgements: This work was partially supported by FCT, Project MAT/34735/99/00.

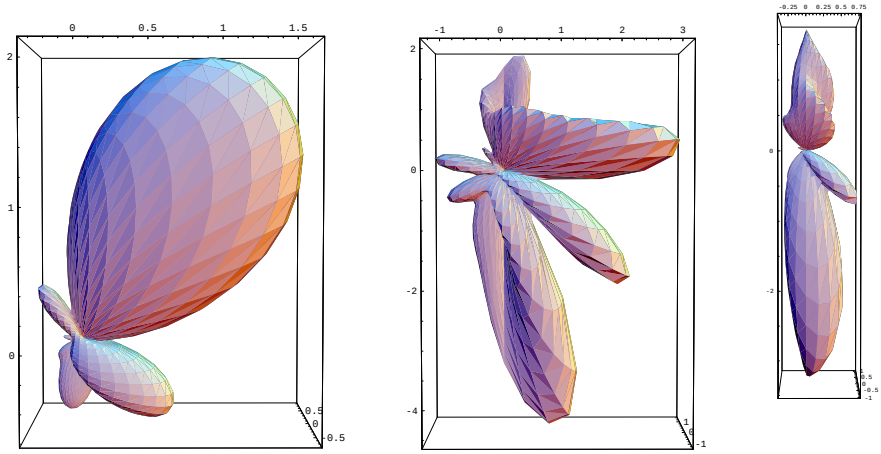

Figure 7: P, SV and SH far field for two elastic disk cracks in parallel planes.

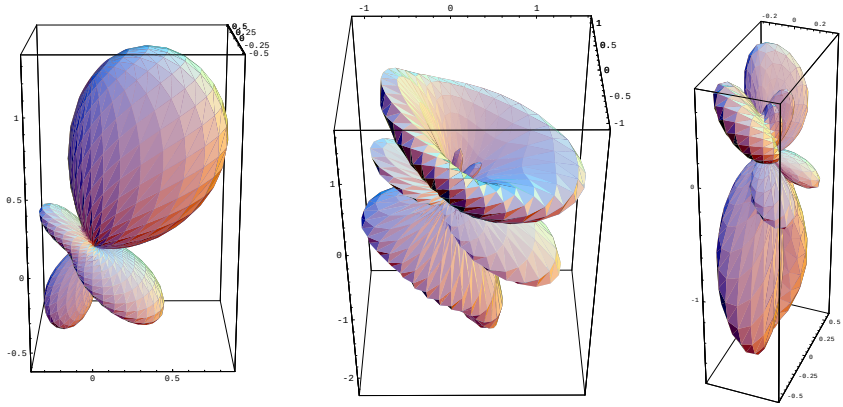

Figure 8: P, SV and SH far field for two elastic elliptic cracks in parallel planes.

References

1. Alves C. J. S., Ha Duong T.: Numerical resolution of the boundary integral equations for elastic scattering by a plane crack, *Int J. Num. Meth. Eng.*, **38**, pp. 2347-2371 (1995)
2. Alves C. J. S., Ha Duong T.: On inverse scattering by screens, *Inverse Problems*, **13**, pp. 1161-1176 (1997)
3. Alves C. J. S. : Numerical simulations on resonance poles, *J. Comp. Appl. Math.*, **111**, pp. 267-279 (1999)
4. Alves C. J. S., Ribeiro P.M.C.: Crack detection using spherical waves and near field measurements, *in Advances in Boundary Elements (Ed: C. Brebbia, H. Power)*, WIT Press, pp. 335-344 (1999)
5. Alves C. J. S., Ha Duong T.: On inverse scattering by elastic cracks, *Inverse Problems*, **15**, pp. 91-97 (1999)
6. Colton D., Kress R.: Inverse acoustic and electromagnetic scattering theory, *Springer-Verlag,* 2nd. ed. (1998)
7. Ha Duong, T.: On the boundary integral equations for the crack opening displacement of flat cracks, *Int. Eq. Op. Th.*, pp. 427-453 (1992)
8. Bécache. E., Ha Duong T. : A spacetime.variational formulation for the boundary integral equation in a 2D elastic crack problem, Math. Meth. Appl. Sc., pp.431-354 (1994)